

## Resonance Raman Spectroscopy of a Light-Harvesting Protein from the Brown Alga *Laminaria saccharina*<sup>†</sup>

A. A. Pascal,<sup>\*,‡</sup> L. Caron,<sup>§</sup> B. Rousseau,<sup>§</sup> K. Lapouge,<sup>‡</sup> J.-C. Duval,<sup>§</sup> and B. Robert<sup>‡</sup>

Section de Biophysique des Protéines et des Membranes, DBCM/CEA & URA 2096/CNRS, CE-Saclay, 91191 Gif-sur-Yvette, France, and Photorégulation et Dynamique des Membranes Végétales, URA 1810/CNRS, ENS, 46 rue d'Ulm, 75230 Paris, France

Received August 8, 1997; Revised Manuscript Received November 5, 1997

**ABSTRACT:** Resonance Raman spectroscopy of an antenna protein from the brown alga *Laminaria saccharina* has been used to investigate the molecular structure of this light-harvesting complex (LHC) at the level of its bound pigments, chlorophylls (chl) *a* and *c* and the xanthophyll fucoxanthin. Evidence has been obtained for the conservation of pigment structure during the isolation procedure used. Six chl *a* and two chl *c* molecules are indicated from the positions and relative contributions of stretching modes of their keto-carbonyl groups. Of special interest is the presence of a population of chls *a* having a protein-binding conformation highly similar to that seen in antenna proteins from higher plants, possibly indicating a common structural motif within this extended gene family. The eight fucoxanthin molecules evidenced are all in the all-trans conformation; however, one or two have a highly twisted configuration. The results are discussed in terms of common and varying structural features of LHCs in higher plants and algae.

The light reactions of photosynthesis in higher plants and algae occur in the thylakoid membranes of specialized organelles called plastids. The organization of this apparatus is complex, involving a large number of membrane proteins containing bound pigment molecules (chlorophylls and carotenoids). Among these, the light-harvesting proteins are responsible for the collection of light energy and its transfer, in the form of excitation energy, to other pigment–proteins called reaction centers where primary charge separation occurs. These light-harvesting complexes are themselves highly organized; the outer antenna of higher plants consists of at least eight distinct proteins, four associated with each photosystem, which form part of the LHC<sup>1</sup> multigene family (1, 2). In addition, each photosystem contains a number of unrelated, inner light-harvesting proteins. The LHC proteins have been the subject of intensive study over recent years, particularly since the publication of an atomic model of the major complex LHCIIb (3). This protein contains three membrane–spanning helices, plus a fourth amphiphilic helix at the membrane–lumen surface, and binds twelve or more chlorophyll molecules plus at least three xanthophylls. It is believed to be present as a trimer *in vivo*, unlike the other plant LHC proteins which are probably monomeric; no data on supramolecular interactions in algal LHCs are currently available.

The genes coding for LHC apoproteins in green plants show a high degree of homology at the level of their amino acid sequence and they are therefore predicted to have the same basic structure (4, 5); their pigment-binding properties are, however, quite different (5, 6). Algal LHCs, among them the fucoxanthin-chlorophyll *a/c*-proteins of brown algae, exhibit a more distant homology with the plant LHC family (7–9). Thus while structural information at the pigment level is still incomplete for LHCIIb, that for the equivalent proteins from algal thylakoids as well as for the minor plant LHCs is at best inadequate, based largely on analogy with this major plant protein. This is particularly true of algal complexes where not only are pigments bound in different proportions but in some cases the pigments themselves are distinct; for example the brown chromophyte algae contain chlorophyll *c* in addition to *a* (no chl *b* is present) and have a very high proportion of the allenic xanthophyll fucoxanthin, which is completely absent in higher plants (10). Unlike chls *a* and *b*, the chlorophyll *c* molecule has a fully unsaturated porphyrin macrocycle and the oscillator strength of its *Q<sub>y</sub>* transition is greatly reduced while that of its Soret transition is increased (11); the fucoxanthin molecule shows a large redshift toward 540 nm when bound to protein (12). It is likely that these differences in pigment composition result from adaptations to differing light qualities; in low-lying marine ecosystems, radiation in the green region of the spectrum is more predominant due to shading by other photosynthetic organisms (13).

Although dichroism analyses of chl *c*-binding antennae have been reported (14), precise details of pigment conformation in algal LHC proteins at a molecular level remain elusive. Recently, advances have been made in the isolation of antenna complexes from a number of algae (15, 16),

<sup>†</sup> A.A.P. was supported by a FEBS postdoctoral fellowship.

<sup>\*</sup> Author to whom correspondence should be addressed.

<sup>‡</sup> Section de Biophysique des Protéines et des Membranes.

<sup>§</sup> Photorégulation et Dynamique des Membranes Végétales.

<sup>1</sup> Abbreviations: chl, chlorophyll; CCD, charge-coupled device; FT, Fourier-transform; fwhm, full width at half-maximum; HPLC, high-performance liquid chromatography; IEF, isoelectric focusing; LHC, light-harvesting complex; OD, optical density; SD, standard deviation.

among them two new fucoxanthin-chl *a/c*-binding fractions from the chromophyte *Pelvetia canaliculata* obtained by non-denaturing IEF (17). The brown and green fractions, labeled bands **a** and **b**, respectively, were found to bind chls *a* and *c* and fucoxanthin with differing stoichiometries; the green band also contained a significant proportion of convertible violaxanthin. While band **a** was composed almost exclusively of a single 22 kDa polypeptide, band **b** contained a number of polypeptides of the same molecular mass (22 kDa) but which were resolvable by denaturing IEF. This new isolation procedure presents for the first time the possibility of studying an algal LHC protein in terms of its pigment conformation. Here we present resonance Raman spectra of the brown, band **a** fraction from the related brown alga *Laminaria saccharina*.

## MATERIALS AND METHODS

Thalli of *L. saccharina* were collected at the seashore near the Biological Station, Roscoff (France). Isolation of the brown light-harvesting fraction (called band **a**) was as described by De Martino et al. (17). In brief, brown algal chloroplasts, prepared by the method of Berkaloff and Duval (18), were disrupted and the suspension solubilized in digitonin, followed by a sucrose-gradient separation to isolate the major LHC fraction (19). The dialyzed, concentrated LHC was then submitted to a non-denaturing IEF procedure (6), and the bands were collected and eluted with a minimum volume of 1% glycine buffer pH 7.

Absorption spectra were recorded at 77 K on an Aminco DW spectrophotometer. Pigment analysis was carried out by reverse-phase HPLC (20); chl *c*<sub>1</sub>/*c*<sub>2</sub> estimation was performed using the same elution profile on a Spherisorb ODS2 column. Chlorophyll *a/c* ratios were determined in 90% acetone according to Jeffrey and Humphrey (21).

Protein samples for Raman spectroscopy were concentrated to an OD in the Soret region of 50–100 (~1 mgchl/mL) in Microcon-30 concentrators (Amicon); isolated pigments were dissolved in a minimum volume of the appropriate solvent. Absorption spectra were taken before and after Raman measurements to verify sample integrity. FT-preresonance Raman spectroscopy was performed at 298 K on a Fourier-transform infrared spectrophotometer (Bruker IFS66) equipped with a Raman module (Bruker FRA106), using 1064 nm excitation from a continuous Nd:YAG laser (22). Resonance Raman spectra at 77 K were obtained in a TBT flow cryostat using a Jobin-Yvon U1000 Raman spectrophotometer equipped with an N<sub>2</sub>-cooled CCD detector, as described previously (23). Excitation was provided by Coherent Argon (Innova 100) and Krypton (Innova 90) lasers (457.9, 476.5, 488.0, 514.5 and 528.7 nm and 406.7 and 413.1 nm, respectively) and a Liconix helium–cadmium laser (441.6 nm).

## RESULTS AND DISCUSSION

Shown in Figure 1 are 77 K absorption spectra of the bulk LHC (dashed line) and the brown IEF band (full line). The non-denaturing IEF procedure has resulted in a sharpening of the principal chl *a* *Q*<sub>y</sub> band at 668 nm and an increase in bands associated with chl *c* (at 633, 588, and 457 nm) and fucoxanthin. It did not, however, perturb the large redshift

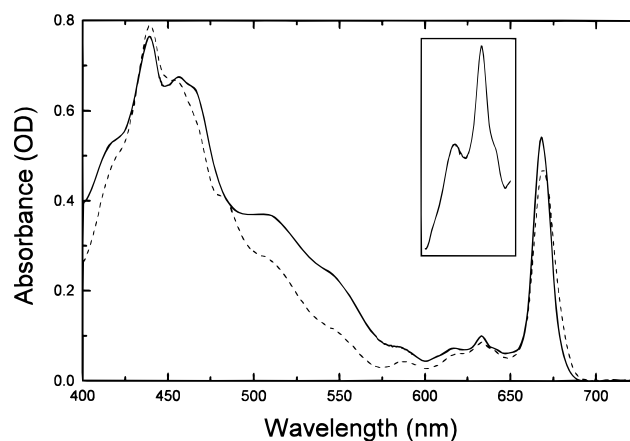


FIGURE 1: 77 K absorption spectra of bulk light-harvesting fraction (dashed line) and band **a** (full line) performed on an Aminco DW spectrophotometer. (Inset) Blowup (8×) of 600–650 nm region for band **a**.

Table 1: Pigment Composition of the LHC Fraction and the Brown IEF Band (band **a**) Determined by Reverse-Phase HPLC (20)<sup>a</sup>

	LHC	band <b>a</b>
chlorophyll <i>a</i>	100.0	100.0
chlorophyll <i>c</i> <sub>1</sub> + <i>c</i> <sub>2</sub>	23.4 (±2.5)	35.9 (±1.5)
chl <i>a/c</i>	4.27 (±0.45)	2.79 (±0.1)
chl <i>c</i> <sub>1</sub> / <i>c</i> <sub>2</sub>	0.64 (±0.02)	0.64 (±0.02)
fucoxanthin	88.1 (±6.0)	126.0 (±1.5)
violaxanthin	9.1 (±1.5)	—
β-carotene	1.0 (±0.15)	—

<sup>a</sup> Chls *c*<sub>1</sub> and *c*<sub>2</sub> were resolved using the same elution profile on a Spherisorb ODS2 column; chl *a/c* ratios were estimated in 90% acetone according to Jeffrey and Humphrey (21). Values represent the mean of four experiments and are expressed in molar percentages (±SD) relative to chl *a* (which includes phaeophytin *a*, 0.7%), or as molar ratios (±SD).

in carotenoid absorption which is observed in bulk LHC; in the spectrum of the brown band absorption of these molecules is observed at 466, 510, and 548 nm, compared with 460, 480, and 510 nm for isolated fucoxanthin in CS<sub>2</sub> (12). These features are consistent with the pigment analysis (Table 1) which indicates a relative increase in fucoxanthin and a reduction in the chl *a/c* ratio. Note that the *Q*<sub>x</sub> and *Q*<sub>y</sub> bands of chls *c* are of similar intensity and are present at 588 and 633 nm, respectively (11); the broad feature around 618 nm corresponds to vibrational overtones of the chl *a* *Q*<sub>y</sub> transition at 668 nm. The shoulder at 641 nm (see inset) may reflect the presence in band **a** of chls *c*<sub>1</sub> and *c*<sub>2</sub>, although this is unlikely as the absorption properties of these pigments are not usually sufficiently different to distinguish between their respective bands (1–2 nm difference in *Q*<sub>y</sub> transition for isolated pigments) (11). Alternatively, this may represent the presence of two chl *c* populations in different environments.

Represented in Figure 2 are the structures of chls *a* and *c*<sub>1</sub> and fucoxanthin. The brown algal protein contains the related chls *c*<sub>1</sub> and *c*<sub>2</sub> (at a ratio of about 2:3; see Table 1). These molecules differ by the nature of the peripheral residue at position 4 on the macrocycle, which is ethyl in the case of chl *c*<sub>1</sub> and vinyl for chl *c*<sub>2</sub>. The exact structural significance of this distribution is unknown, but the absorption properties of both molecules are almost identical (11). As mentioned above, unlike chl *a* (and *b*) the chlorophyll *c* molecule has a fully unsaturated porphyrin macrocycle,

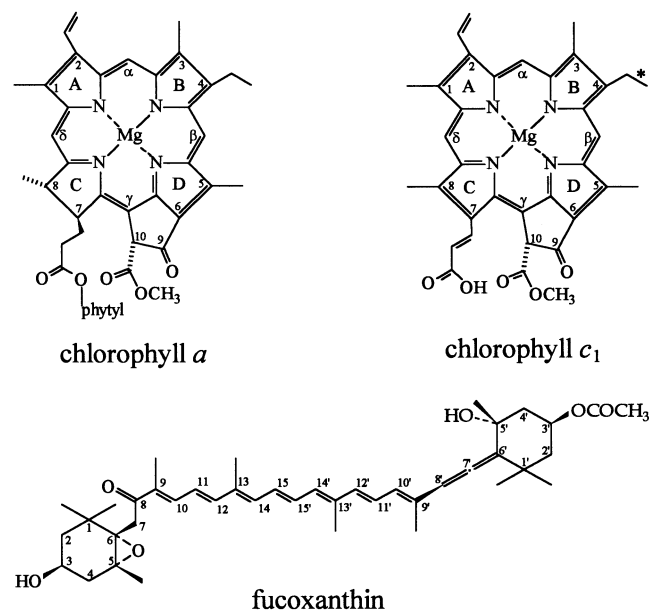


FIGURE 2: Molecular structure of chlorophyll *a*, chlorophyll *c*<sub>1</sub>, and fucoxanthin. Chlorophyll *c*<sub>2</sub> contains a carbon-carbon double bond at the position marked by an asterisk (from refs 11, 24, 25).

resulting in an increase in symmetry relative to chl *a* and thus conferring different absorption and vibrational properties. The most obvious difference between chls *c* and *a* concerns the intensity of the  $Q_y$  transition, which is greatly reduced for chl *c* with respect to chlorophylls containing a chlorin ring (11). To analyze resonance Raman spectra of algal LHCs, precise vibrational information on isolated chl *c* is required. FT-Raman spectra of chl *c* extracts from *Laminaria* LHC (thus containing chls *c*<sub>1</sub> and *c*<sub>2</sub> in similar proportions) were therefore performed. As discussed in detail elsewhere (26, 27), Raman mode frequencies do not change as a function of temperature or excitation wavelength (in the absence of associated conformational changes), while their relative intensities may vary. Thus, although these spectra are recorded at room temperature and in preresonance with the  $Q_y$  transition, the observed band frequencies may be directly compared with those of protein-bound pigments observed at low temperature under Soret resonance (see below).

Vibrational spectra of chl *c* show many similarities with heme *b*, exhibiting in particular a very intense band at 1360  $\text{cm}^{-1}$  under resonance conditions with the Soret electronic transition (K. Lapouge et al., unpublished data), corresponding to the C-N breathing mode (28). Figure 3 shows FT-preresonance Raman spectra in the region 1580–1760  $\text{cm}^{-1}$  of the isolated chls *a*, *b*, and *c* in dry THF, a solvent which provides two external ligands to their central Mg atom but which does not interact with their conjugated carbonyl groups (29). In this region modes corresponding to the methine bridges of the ring are seen around 1600  $\text{cm}^{-1}$ , along with stretching modes of conjugated vinyl groups around 1625  $\text{cm}^{-1}$  and of conjugated carbonyl groups at 1650–1750  $\text{cm}^{-1}$  (29, 30). This region thus contains most of the vibrational modes commonly used for studying (bacterio)chlorophyll interactions in vivo (31). The position of the methine bridge stretching mode is sensitive to the conformation of chlorophyll and bacteriochlorophyll, and it has been extensively used as a fingerprint of the number of axial ligands bound to the central Mg of these molecules (31–33). For chl *c* in

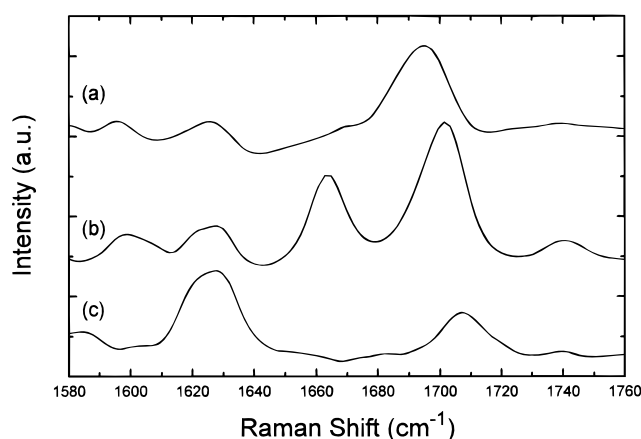


FIGURE 3: FT-preresonance Raman spectra of isolated chlorophylls *a*, *b*, and *c* (a mixture of chls *c*<sub>1</sub> and *c*<sub>2</sub>) in THF [(a)–(c), respectively], obtained as described previously (22).

preresonance with the  $Q_y$  transition, this band is not observed, probably due to the change in molecular symmetry mentioned above which results in these modes being Raman-inactive. Indeed in  $Q$ -band resonance Raman spectra of porphyrin molecules such as heme *b*, these modes are very weak at best (28). The 1625  $\text{cm}^{-1}$  band for chl *c* is more intense, as expected for molecules containing one or two more conjugated vinyl groups than chls *a* and *b* (see Figure 2). A very important parameter which can be deduced from these spectra is the position of the band arising from the stretching mode of the free-from-interaction 9-keto-carbonyl group for each molecule. It was shown in early studies (30) that this band, usually observed at around 1700  $\text{cm}^{-1}$  when the keto-carbonyl group is free from interactions, shifts down toward 1650  $\text{cm}^{-1}$  when this group is involved in intermolecular interactions. The magnitude of this shift is indicative of the strength of the interaction, and this may be estimated from the position of the C=O stretching mode (34). To study chl *c*–protein interactions in vivo, it is thus necessary to determine accurately the position of this band when the keto C=O group is free from interactions. It is worth noting that for each chl molecule the position of this band is different, that is, 1695, 1701, and 1707  $\text{cm}^{-1}$  for chls *a*, *b*, and *c*, respectively (Figure 3). It should be emphasized that the frequency of the 9-keto stretching mode for chl *c* is 12  $\text{cm}^{-1}$  higher than that for chl *a* in similar conditions. Chl *b* also contains a conjugated formyl-carbonyl group at position 3 of the chlorin ring (24; see Figure 2); its stretching frequency is at 1663  $\text{cm}^{-1}$  when free from interactions (Figure 3b). In Figure 3, the width of the band (fwhm) arising from the keto-carbonyl stretching mode is no larger for chl *c* than for chl *a* or *b*, although FT-Raman spectra in this case were obtained from a mixture of chls *c*<sub>1</sub> and *c*<sub>2</sub>. This is a clear indication that the structural difference between the two chls *c* does not have a large influence on the keto-carbonyl stretching mode and thus, from a Raman point of view, these two types of molecule will behave as a single molecular species.

The same region for band *a* is shown in Figure 4 for four different excitations in the Soret region (457.9, 441.6, 413.1, and 406.7 nm), allowing a distinction of the individual chlorophyll contributions (carotenoids exhibit no Raman bands in this region). Because of the different positions of the Soret electronic transition of chl *a* and chl *c*, at 457.9

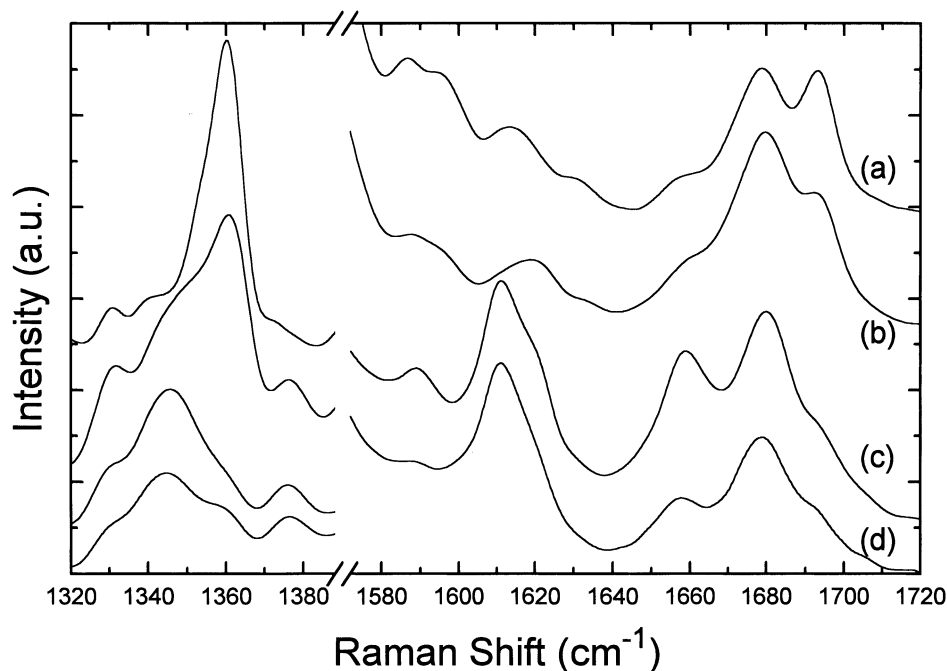


FIGURE 4: 77 K resonance Raman spectra of the band *a* protein excited at 457.9, 441.6, 413.1, and 406.7 nm [(a)–(d), respectively], obtained as described previously (23). Right-hand region (1560–1720  $\text{cm}^{-1}$ ) multiplied by a factor of 2 with respect to left-hand region (1320–1400  $\text{cm}^{-1}$ ).

nm contributions from chl *c* molecules are expected to dominate resonance Raman spectra, while both molecular species should contribute at 441.6 nm, and chl *a* contributions should be dominant at 413.1 and 406.7 nm. This is indeed the case as deduced from analysis of medium-frequency vibrational modes, which may be used as fingerprints for the chemical nature of molecules contributing to the spectra. Thus in Figure 4 the 1360  $\text{cm}^{-1}$  band mentioned above is very strong for excitation at 457.9 nm and is still present at 441.6 nm, whereas at shorter excitation wavelengths (413.1 and 406.7 nm) it is barely visible and corresponds to the same C–N breathing mode of chl *a*. At 457.9 nm (Figure 4a), the presence of two bands arising from the stretching modes of keto-carbonyl groups are discerned at 1679 and 1693  $\text{cm}^{-1}$ . Relative to the frequency of the keto-carbonyl group of chl *c* when free from interactions, which is observed at 1707  $\text{cm}^{-1}$  (see above), these bands are downshifted by 28 and 14  $\text{cm}^{-1}$ , respectively. It can thus be concluded that this protein contains two populations of chl *c*. The keto-carbonyl of one of these populations vibrates at 1679  $\text{cm}^{-1}$  and is thus involved in a medium-strength H-bond ( $\sim 14$  kJ/mol; 34) with its surrounding peptidic environment, while that of the other vibrates at 1693  $\text{cm}^{-1}$ , i.e. either in a rather polar environment or being involved in a weak intermolecular interaction.

It is clearly tempting to correlate these two populations with the two apparent chl *c*  $Q_y$  absorption bands seen in Figure 1, particularly given the role of H-bonding in bacterial antenna proteins in tuning absorption properties (31). The existence of an H-bond between an amino acid side chain and the acetyl-carbonyl group of Bchl *a* induces a redshift of its  $Q_y$  electronic transition, of up to 10 nm for Bchls not involved in strong excitonic interactions (35) or up to 15 nm when these molecules are strongly excitonically coupled (36, 37). However, this was shown to be true for this particular carbonyl group only; H-bonding to the keto-

carbonyl group of Bchl had at best very little effect on its red-most electronic transition (36). Tuning the electronic absorption properties of chl *c* by modulation of intermolecular interactions with their keto-carbonyl would thus indicate that the influence of such H-bonds on their electronic properties is definitely different. However, it has also recently been shown that a change in the electromagnetic properties of the protein-binding site could account for a redshift of the Bchl *a*  $Q_y$  transition of about 150  $\text{cm}^{-1}$  (35). The 1693  $\text{cm}^{-1}$  frequency observed for one population of chl *c* could well account for the presence of a free-from-interaction keto-carbonyl group but which is located in a rather polar environment. The 8 nm shift between the  $Q_y$  of each chl *c* bound to the complex could thus originate from such a difference between the binding sites or from a combination of different dielectric constants and different intermolecular interactions. Alternatively, if the shoulder at 641 nm does not reflect the absorption band of a separate chl *c* population then this would indicate a behavior of this chlorophyll similar to that of Bchl *a*, i.e., that an H-bond to its keto-carbonyl has little effect on its  $Q_y$  electronic transition.

Excitation at 441.6 nm (Figure 4b) produces Raman spectra containing modes of both chls *a* and *c* (as well as carotenoid), as this laser line is situated within the Soret absorption band of both pigments. In addition to the two carbonyl modes corresponding to chl *c*, a third band is seen at 1659  $\text{cm}^{-1}$  which can thus be attributed to a chl *a* molecule (note that a minor contribution from this band is also seen at 457.9 nm; Figure 4a). The positions of the two main bands do not appear to be superimposable on those seen at 457.9 nm, indicating the presence of further keto-carbonyl modes of chl *a* molecules. These contributions are also responsible for the width of the 1680  $\text{cm}^{-1}$  band at this wavelength, which is rather large for a single species (18  $\text{cm}^{-1}$  fwhm, as compared with about 13  $\text{cm}^{-1}$  expected for a single carbonyl



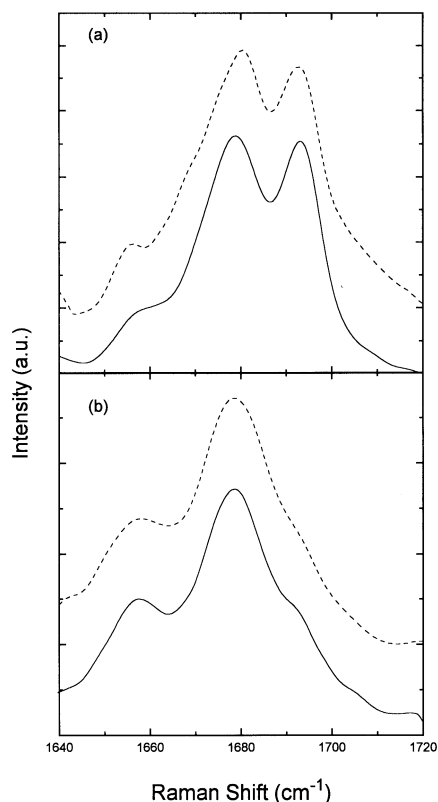


FIGURE 5: 77 K resonance Raman spectra of band **a** (full lines) and the bulk LHC fraction (dashed lines) excited at 457.9 nm (a) and 406.7 nm (b).

vibrator; 30). At higher energy excitation wavelengths (406.7 and 413.1 nm; Figure 4c,d, respectively), where contributions from chl *a* dominate, spectra contain a very broad contribution centered at 1680 cm<sup>-1</sup> together with two bands at 1659 and 1692 cm<sup>-1</sup>. One population of chl *a* has thus a keto group free from interactions (vibrating at 1692 cm<sup>-1</sup>); about a third of the chls *a* present have a keto-carbonyl implicated in a strong H-bond with their protein environment (1659 cm<sup>-1</sup>); and the majority of chls *a* possess a carbonyl vibrating between 1675 and 1685 cm<sup>-1</sup>, i.e. either taking part in an interaction weaker than about 14 kJ/mol (34) vibrating at 1675 cm<sup>-1</sup> or free from interactions in a rather polar environment (vibrating at 1685 cm<sup>-1</sup>).

Given the chl *a/c* ratio of this complex and the relative areas of each carbonyl band observed at 406 and 413 nm, along with the known structure of the related plant protein LHCIIb (which contains seven chl *a* molecules per monomer), a likely estimation is that each monomeric protein contains two chl *c* molecules (each with a distinct carbonyl stretching mode) plus six chls *a* present in three populations. Taking into account the intensities of the non-equivalent bands arising from the 9-keto groups of non-equivalent chls *a*, we propose that three of these molecules have a keto group vibrating between 1675 and 1685 cm<sup>-1</sup>, two correspond to the 1659 cm<sup>-1</sup> band, and one has its carbonyl mode at 1692 cm<sup>-1</sup>.

Presented in Figure 5 are the keto-carbonyl stretching modes (1640–1720 cm<sup>-1</sup>) of band **a** (full lines) compared with those of the bulk LHC from which it was isolated (dashed lines), at two excitations (457.9 and 406.7 nm) which yield information on the interaction states of chl *c* and *a* molecules, respectively (see above). All the bands present

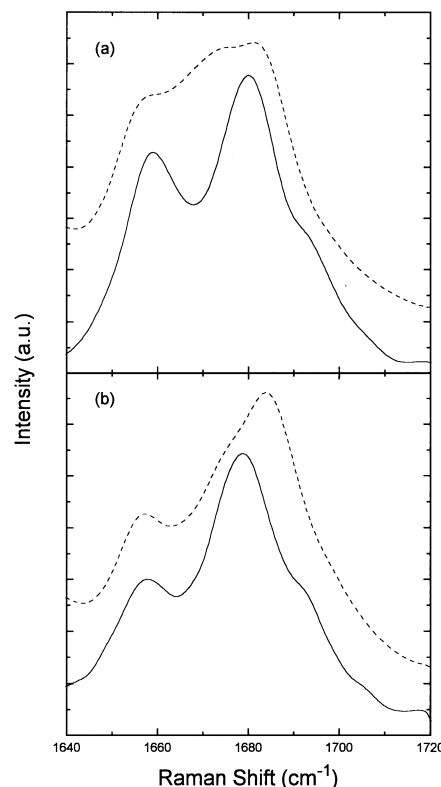


FIGURE 6: 77 K resonance Raman spectra of band **a** (full lines) and LHCIIb from *Spinacia oleracea* (L.) var. *subito* (dotted lines) excited at 413.1 nm (a) and 406.7 nm (b). LHCIIb was obtained as described by Ruban et al. (6).

in the brown fraction are clearly observed in the whole LHC, indicating that the IEF procedure has not resulted in the appearance of new bands at different frequencies. It can thus be concluded that no chlorophyll–protein interactions present in the bulk complex have been disrupted. This is a good indication that the state of the protein has not been adversely affected by the isolation procedure. However, an additional shoulder near 1670 cm<sup>-1</sup> (457.9 nm excitation) indicates the presence, in the whole LHC, of populations of chl *c* other than those observed in band **a**. The lack of additional major bands for the bulk LHC and the similarity of resonance Raman spectra between the two samples both in terms of band position and relative intensity are also worthy of note and strongly suggest that the band **a** protein is the major complex present in the LHC fraction. However, if other complexes exist in the whole LHC whose chlorophyll-binding sites are similar to those of band **a**, their presence could result in spectra similar to those observed in Figure 5.

It is of interest to compare the interactions provided by the chl *a* binding sites in both algal and higher plant proteins in order to observe whether there could be any similarity between them which could in turn reflect structural similarities between these proteins. In Figure 6 are presented the chl *a* carbonyl modes of band **a** (full lines) together with those of the plant antenna protein LHCIIb (dotted lines) for the two excitations yielding specific information on chl *a* interactions (i.e. 413.1 and 406.7 nm). In the spectra of both of these distantly related proteins, the band arising from keto-carbonyl groups involved in strong H-bonding interactions at 1659 cm<sup>-1</sup> is present. This observation indicates a similarity in protein interaction of the corresponding pigments which, given that the interaction involved is strong (rather

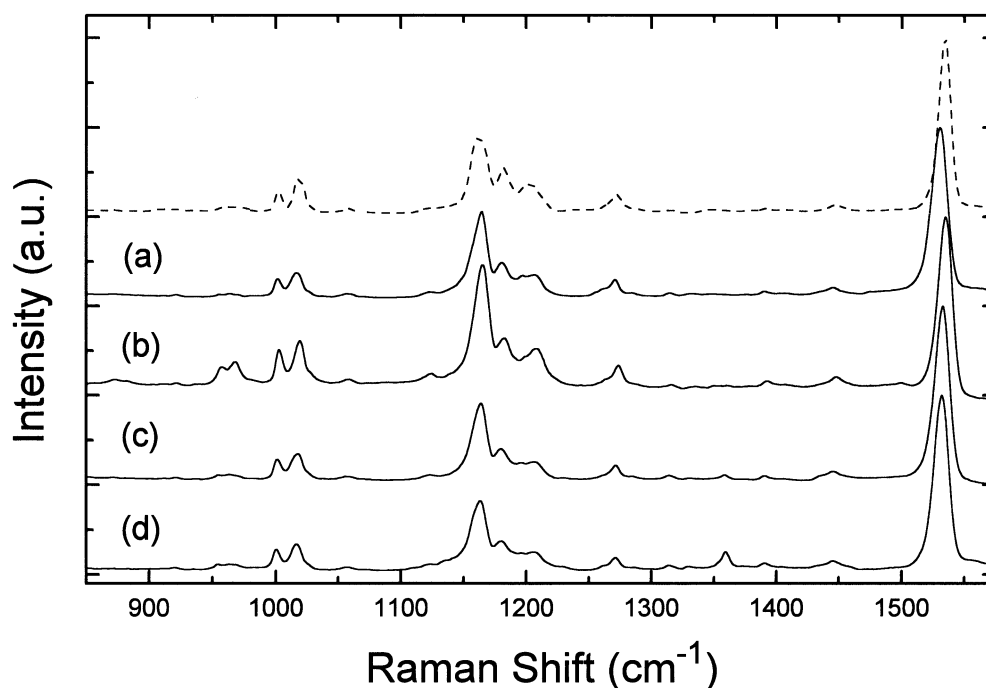


FIGURE 7: 77 K carotenoid resonance Raman spectra of band **a** excited at 528.7, 514.5, 488.0, and 476.5 nm [(a)–(d), respectively]. Also shown is the spectrum of isolated all-trans fucoxanthin in cyclohexane, excited at 514.5 nm (dashed line).

than a free-from-interaction carbonyl which may be reproduced in many unrelated chl–proteins), points to a possible similarity in structure of one or two chl-binding pockets. This may thus represent a common structural feature within this extended gene family. The same mode is also observed for the minor plant protein CP29 (A. A. Pascal et al., unpublished results), and we are currently analyzing resonance Raman spectra of other members of the LHC family in order to verify how far this conclusion can be extended. Note that similarities in chlorophyll spatial arrangements between LHCs of plants and algae for at least some of the chl molecules present has already been implied from dichroism studies (14, 38, 39).

In addition to chlorophyll molecules, resonance Raman spectra can be obtained for the other pigment present in the complex, namely, the xanthophyll fucoxanthin. Figure 7 presents such spectra for the band **a** protein for a range of excitations between 476.5 and 528.7 nm, along with a spectrum of isolated all-trans fucoxanthin in cyclohexane obtained by excitation at 514.5 nm (dashed line). Fucoxanthin is an allenic carotenoid, and, as such, its resonance Raman spectra are very similar to that of more classical carotenoids such as  $\beta$ -carotene, which has been extensively studied (40) and its modes empirically calculated (41). As in the resonance Raman spectra of  $\beta$ -carotene, four major groups of bands are present in the spectra of fucoxanthin (called  $\nu_1$ – $\nu_4$ ), one additional band being observed in the  $\nu_3$  region (around 1020  $\text{cm}^{-1}$ ) which could arise from rocking modes of the methyl group on  $\text{C}_9$ , coupled with the unusual conjugated  $\text{C}=\text{O}$  group at position 8 (dashed line, Figure 7; see Figure 2). Comparison of the resonance Raman spectra of isolated, all-trans fucoxanthin with fucoxanthin in band **a** reveals unambiguously that all xanthophylls bound to this protein are in the all-trans conformation. Upon trans  $\rightarrow$  cis isomerization, as is well-documented for  $\beta$ -carotene (40, 41) and has been verified for fucoxanthin (A. A. Pascal et al., unpublished results), the position of the major  $\nu_1$  mode at

1530  $\text{cm}^{-1}$  upshifts (for 13-cis-fucoxanthin, for example, this band is upshifted by more than 10  $\text{cm}^{-1}$ ; not shown) and at the same time the resulting change in molecular symmetry often induces the presence of additional modes, each of them characteristic of a specific conformation (40, 41). It may thus be safely concluded, in the absence of such an observation, that all the fucoxanthin molecules bound to the protein of band **a** are in the all-trans configuration.

When band **a** is excited at 514.5 nm, the intensity of the very weak modes around 956 and 966  $\text{cm}^{-1}$  (the  $\nu_4$  region) increases dramatically. These bands arise from out-of-plane modes involving torsion around  $\text{C}=\text{C}$  bonds, as well as out-of-plane motions of the chain hydrogen atoms (41). Note that this increase in intensity cannot be merely a resonance effect, as no similar increase was observed upon varying excitation conditions for the isolated pigment (not shown). Similar effects have been observed for the spheroidene molecule bound to reaction centers of purple bacteria, and these were safely attributed to the presence of a twisted configuration of this carotenoid, i.e. a carotenoid possessing a torsion around a carbon–carbon single bond (42). This twisting decreases the molecular symmetry of the conjugated molecule so that out-of-plane modes, which are formally forbidden in  $\text{C}_{2h}$  symmetry, become allowed. It was further observed that this twisted configuration had no effect on the frequency of the other modes of this carotenoid (42). In the case of bacterial reaction centers, as discussed by Arnoux et al. (43), the molecular configuration of the carotenoid deduced from Raman spectroscopy was fully confirmed by X-ray crystallography.

Considering the close similarity between fucoxanthin and  $\beta$ -carotene resonance Raman spectra, it may be safely concluded that these modes reveal the presence of a population of fucoxanthin molecules which is in a twisted configuration, although nevertheless all-trans (as the frequency of their  $\nu_1$  band is not modified relative to all-trans fucoxanthin). Such a twisted all-trans configuration has until

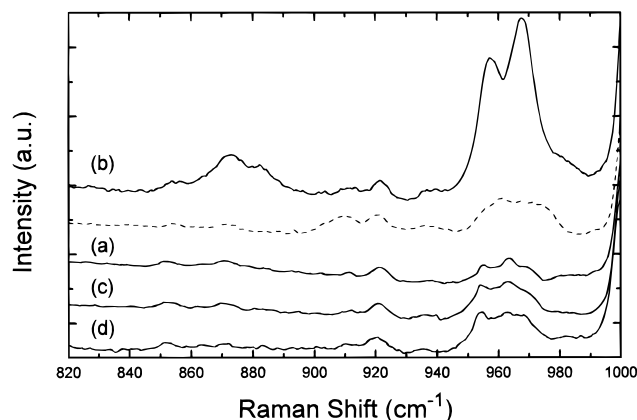


FIGURE 8: Expansion of  $\nu_4$  region (820–1000  $\text{cm}^{-1}$ ) from Figure 7 (note that trace b has been displaced to the top of the figure).

now never been observed for a carotenoid molecule bound to a photosynthetic protein. At lower frequencies, other bands which also arise from out-of-plane motions (873 and 882  $\text{cm}^{-1}$ ) similarly gain intensity at 514.5 nm (Figure 8). According to mode calculations performed for all-trans  $\beta$ -carotene (41), in this region bands arising from out-of-plane wagging localized near the  $\text{C}_{10}$  and  $\text{C}_{14}$  (and  $\text{C}_{10'}$  and  $\text{C}_{14'}$ ) atoms will principally contribute. However, recently selective deuteration of spheroidene when bound to the reaction centers of *Rhodobacter sphaeroides* has indicated that care should be taken when considering conclusions drawn from the comparison of resonance Raman data on this molecule with normal mode calculations performed on  $\beta$ -carotene (44). In particular, the lower molecular symmetry of spheroidene seems to induce significant differences in the precise localization of the modes participating in the observed Raman bands. As fucoxanthin is structurally less-related to  $\beta$ -carotene than spheroidene, precise localization of the molecular twist induced by binding to the band a protein would require more detailed analysis of this particular carotenoid.

Although the number of these molecules is difficult to estimate from the Raman measurements, the fact that this population is observed only at 514.5 nm excitation indicates that only a few molecules per complex are in such a configuration. On the basis of the pigment composition of this protein an estimation can be made of the number and distribution of fucoxanthin molecules per protein. Given six chls *a* per monomer (see above), there would be approximately eight fucoxanthins bound to the apoprotein, of which probably one or two are involved in the twisting described above.

The fucoxanthin-chl *a/c*-binding protein studied here shows clear similarities to the LHC proteins from higher plants, particularly in chl-binding stoichiometries and in the apparent presence of a population of chls *a* having binding sites structurally related to these antenna proteins. The presence of other antenna proteins in brown algae, evidenced by the complexity of a second IEF band (band b; 17), may also indicate a polypeptide complexity similar to that of the higher plant LHC family (cf. ref 15). By contrast, the protein studied here contains much higher stoichiometric amounts of its bound xanthophyll (in this case fucoxanthin) than that seen in the plant antennae. The exact nature and position of the binding of such a large number of carotenoids to a

relatively small apoprotein (22 kDa) remains an area for further investigation, as does the role of the twisted fucoxanthin molecules evidenced by differential excitation. In addition, the absorption properties of the two chlorophyll *c* populations are currently under investigation.

## ACKNOWLEDGMENT

We thank Christine Pourcet for the FT-preresonance Raman spectra of chlorophylls *a* and *b*.

## REFERENCES

1. Jansson, S. (1994) *Biochim. Biophys. Acta* 1184, 1–19.
2. Green, B. R., and Durnford, D. G. (1996) *Annu. Rev. Plant Physiol. Plant Mol. Biol.* 47, 685–714.
3. Kühlbrandt, W., Wang, D. N., and Fujiyoshi, Y. (1994) *Nature* 367, 614–621.
4. Pichersky, E., Subramaniam, R., White, M. J., Reid, J., Aebersold, R., and Green, B. R. (1991) *Mol. Gen. Genet.* 227, 277–284.
5. Thornber, J. P., Peter, G. F., Morishige, D. T., Gómez, S., Anandan, S., Welty, B. A., Lee, A., Kerfeld, C., Takeuchi, T., and Preiss, S. (1993) *Biochem. Soc. Trans.* 21, 15–18.
6. Ruban, A. V., Young, A. J., Pascal, A. A., and Horton, P. (1994) *Plant Physiol.* 104, 227–234.
7. Apt, K. E., Clendennen, S. K., Powers, D. E., and Grossman, A. R. (1995) *Mol. Gen. Genet.* 246, 455–464.
8. Caron, L., Douady, D., Quinet-Szely, M., de Goër, S., and Berkaloff, C. (1996) *J. Mol. Evol.* 43, 270–280.
9. Durnford, D. G., Aebersold, R., and Green, B. R. (1996) *Mol. Gen. Genet.* 253, 377–386.
10. Hiller, R. G., Anderson, J., and Larkum, A. W. D. (1991) in *Chlorophylls* (Scheer, H., Eds.) pp 529–547, CRC Press, Boca Raton, FL.
11. Jeffrey, S. W. (1989) in *Chromophyte Algae: Problems and Perspectives* (Green, J. C., Leadbetter, B. S. C., and Diver, W. L., Eds.) pp 13–36, Clarendon Press, Oxford, U.K.
12. Kirk, J. T. O. (1977) *Plant Sci. Lett.* 9, 373–380.
13. Larkum, A. W. D. (1991) in *Chlorophylls* (Scheer, H., Ed.) pp 367–383, CRC Press, Boca Raton, FL.
14. Büchel, C., and Garab, G. (1997) *J. Photochem. Photobiol.* 37, 118–124.
15. Durnford, D. G., and Green, B. R. (1994) *Biochim. Biophys. Acta* 1184, 118–123.
16. Jovine, R. V. M., Johnsen, G., and Prézélin, B. B. (1995) *Photosynth. Res.* 44, 127–138.
17. De Martino, A., Douady, D., Rousseau, B., Duval, J.-C., and Caron, L. (1997) *Photochem. Photobiol.* 66, 190–197.
18. Berkaloff, C., and Duval, J.-C. (1980) *Photosynth. Res.* 1, 127–135.
19. Passaquet, C., Thomas, J. C., Caron, L., Hauswirth, N., Puel, F., and Berkaloff, C. (1991) *FEBS Lett.* 280, 21–26.
20. Arsalane, W., Rousseau, B., and Duval, J.-C. (1994) *Photochem. Photobiol.* 60, 237–243.
21. Jeffrey, S. W., and Humphrey, G. F. (1975) *Biochem. Physiol. Pflanz.* 167, 191–194.
22. Mattioli, T. A., Hoffmann, A., Robert, B., Schrader, B., and Lutz, M. (1991) *Biochemistry* 30, 4648–4654.
23. Sturgis, J. N., and Robert, B. (1994) *J. Mol. Biol.* 238, 445–454.
24. Scheer, H. (1991) in *Chlorophylls* (Scheer, H., Ed.) pp 1–30, CRC Press, Boca Raton, FL.
25. Bernhard, K., Moss, G. P., Tóth, G., and Weedon, B. C. L. (1976) *Tetrahedron Lett.* 1976, 115–118.
26. Ivancich, A., Lutz, M., and Mattioli, T. M. (1997) *Biochemistry* 36, 3242–3253.
27. Sturgis, J., and Robert, B. (1997) *J. Phys. Chem. B* 101, 7227–7231.
28. Spiro, T. G. (1983) in *Iron Porphyrins* (Lever, A. B. P., and Gray, H. B., Eds.) Part 2, pp 89–159, Addison-Wesley, Reading, MA.
29. Feiler, U., Mattioli, T. A., Katheder, I., Scheer, H., Lutz, M., and Robert, B. (1994) *J. Raman Spectrosc.* 25, 365–370.

30. Lutz, M. (1984) in *Advances in IR and Raman Spectroscopy* (Clark, R. J. H., and Hester, R. E., Eds.) pp 211–300, John Wiley and Sons, New York.
31. Robert, B. (1996) in *Biophysical Techniques in Photosynthesis* (Amesz, J., and Hoff, A. J., Eds.) pp 161–176, Kluwer, Dordrecht, The Netherlands.
32. Cotton, T. M., and van Duyne, R. P. (1981) *J. Am. Chem. Soc.* 103, 6020–6026.
33. Näveke, A., Lapouge, K., Sturgis, J. N., Hartwich, G., Simonin, I., Scheer, H., and Robert, B. (1997) *J. Raman Spectrosc.* 28, 599–604.
34. Zhadorozhnyi, B. A., and Ishchenko, I. K. (1965) *Opt. Spectrosc. (Engl. Transl.)* 19, 306–308.
35. Gall, A., Fowler, G. J. S., Hunter, C. N., and Robert, B. (1997) *Biochemistry* (in press).
36. Sturgis, J. N., Jirzakowa, W., Reiss-Husson, F., Cogdell, R. J., and Robert, B. (1995) *Biochemistry* 34, 517–523.
37. Sturgis, J. N., Olsen, J. D., Robert, B., and Hunter, C. N. (1997) *Biochemistry* 36, 2772–2778.
38. Mimuro, M., Katoh, T., and Kawai, H. (1990) *Biochim. Biophys. Acta* 1015, 450–456.
39. Hiller, R. G., and Breton, J. (1992) *Biochim. Biophys. Acta* 1102, 365–370.
40. Koyama, Y., Takii, T., Saiki, K., and Tsukida, K. (1983) *Photobiochem. Photobiophys.* 5, 139–150.
41. Saito, S., and Tasumi, M. (1983) *J. Raman Spectrosc.* 14, 310–321.
42. Lutz, M., Szponarski, W., Berger, G., Robert, B., and Neumann, J.-M. (1987) *Biochim. Biophys. Acta* 894, 423–433.
43. Arnoux, B., Ducruix, A., Reiss-Husson, F., Lutz, M., Norris, J., Schiffer, M., and Chang, C.-H. (1989) *FEBS Lett.* 258, 47–50.
44. Kok, P., Köhler, J., Groenen, E. J. J., Gebhard, R., van der Hoef, I., Lugtenburg, J., Farhoosh, R., and Frank, H. (1997) *Spectrochim. Acta* 53A, 381–392.

BI9719657